Young adult lung adenocarcinoma with bilateral multiple microcystic pulmonary lesions highly suspicious for metastasis: a case report

Qin Jian[1#], Di Xu[1#], Min Liu[1], Bingzhu Hu[1], Chenghong Li[1*]

# These authors contributed equally to this work and share first authorship.

European Journal of Medical Case Reports
Volume XX(XX):01–08
DOI: XXXX

ABSTRACT

Background: Bilateral multiple microcystic pulmonary lesions highly suspicious for metastasis are a rare radiological manifestation of lung adenocarcinoma and have seldom been reported in young adults. Such lesions are easily misinterpreted as infectious or cystic lung diseases, potentially leading to delayed diagnosis and inappropriate management. We report a case of lung adenocarcinoma in a young welder with multifactorial risk factors who presented with bilateral multiple microcystic lesions and achieved a sustained response to osimertinib, aiming to improve recognition and timely management of this rare presentation.

Case presentation: A 35-year-old Chinese male welder presented with cough and blood-streaked sputum. Chest computed tomography (CT) revealed a left lower lobe mass, mediastinal and left supraclavicular lymphadenopathy, and bilateral multiple microcystic lesions highly suspicious for metastasis. Despite anti-infective therapy, the pulmonary lesions persisted, and biopsy confirmed lung adenocarcinoma harboring an epidermal growth factor receptor exon 19 deletion and a somatic TP53 co-mutation (programmed death-ligand 1 tumor proportion score 10%). Osimertinib 80 mg daily achieved an ongoing partial response sustained at 9 months (−58.0%), with no significant adverse events.

Conclusions: This case highlights that bilateral multiple microcystic pulmonary lesions in a young patient with risk factors should raise suspicion of metastatic involvement from lung adenocarcinoma, prompting timely pathological biopsy and genetic testing for timely diagnosis. In this patient, 9 months of osimertinib therapy achieved a sustained radiological response despite the concurrent TP53 mutation, suggesting that TP53 co-mutation did not preclude response in this patient, although this single case cannot be generalized.

Keywords: Young adult lung adenocarcinoma, metastasis, EGFR mutation, TP53, welder, targeted therapy, diagnostic challenge.

Type of Article: Case Report **Specialty:** Oncology

Correspondence to: Chenghong Li
*Department of Pulmonary and Critical Care Medicine, Affiliated Hospital of Jianghan University, Wuhan, Hubei, China.
Email: 15827636399@163.com
Full list of author information is available at the end of the article.

Received: 13 July 2026
Revised (1): 02 September 2026
Accepted: 11 September 2026

Introduction

Lung cancer remains the leading cause of cancer-related death worldwide, with an increasing incidence in certain populations and a trend toward younger age at onset [1–3]. Non-small cell lung cancer (NSCLC) is highly heterogeneous. Its main subtype, lung adenocarcinoma, usually gives rise to solid nodules in the lung or pleural metastases [4–5]. Bilateral multiple microcystic pulmonary lesions, a rare radiological manifestation highly suspicious for pulmonary metastasis, have rarely been reported [6]. Because they mimic bronchiectasis, infections, or cystic lung diseases, such lesions can be misinterpreted, leading to delayed diagnosis and treatment [7].

Young adults with lung cancer and occupationally related lung cancer are getting more attention lately. Welding fumes are a Group 1 carcinogen, according to the International Agency for Research on Cancer (IARC), and long-term exposure raises lung cancer risk [8]. We report the case of a 35-year-old Chinese male welder with lung adenocarcinoma who presented with bilateral multiple microcystic pulmonary lesions highly suspicious for metastasis. The clinical, imaging, pathological, and molecular features are described, along with a review of the relevant literature, to raise awareness of this uncommon presentation and facilitate timely diagnosis.

Case Presentation

Chief complaint and history

On December 1, 2025, we admitted a 35-year-old Chinese man. He had been coughing and producing sputum for

more than a month, with small amounts of white or grayish sputum and no clear trigger. One day before admission, his cough worsened, and he developed low-grade fever, blood-streaked sputum, and dyspnea on exertion. Chest computed tomography (CT) at an outside hospital suggested bilateral pulmonary infection and widespread bilateral diffuse microcystic opacities. He was treated with intravenous moxifloxacin (0.4 g once daily) for 10 days, but his symptoms did not improve and he was referred to our hospital.

Past medical history

The patient was previously healthy. He denied any history of malignancy, chronic respiratory diseases (including pulmonary tuberculosis), hypertension, diabetes mellitus, coronary heart disease, or viral hepatitis.

He had smoked for 17 years (20 cigarettes, i.e., 1 pack, per day; 17 pack-years). He had worked as a welder in a factory for 17 years, approximately 10 hours per day, mainly welding carbon steel, with occasional stainless steel welding involving potential exposure to hexavalent chromium and nickel. He wore only an ordinary gauze mask, which provides minimal protection against welding fumes, and never used a particle-filtering respirator or a powered air-purifying respirator; the workshop was equipped with general ventilation only.

His three maternal uncles were all long-term smokers (>30 years) and were respectively diagnosed with lung cancer at the ages of 58, 66, and 70 years, and histological types are unknown.

Physical examination

On admission, his vital signs were as follows: body temperature 36.0°C, pulse 68 beats/minute, respiratory rate 21/minute, and blood pressure 135/62 mmHg. We palpated a left supraclavicular lymph node about 1.5 cm in size; it was firm, mobile, non-tender, and well-defined. Breath sounds were coarse bilaterally, without rales. Cardiac and abdominal examinations were unremarkable, and there was no lower limb edema.

Laboratory testing

Laboratory findings showed elevated hypersensitive C-reactive protein (45.22 mg/l) and interleukin-6 (16.87 pg/ml). Liver and kidney function, coagulation parameters, erythrocyte sedimentation rate, and tumor markers (carcinoembryonic antigen, neuron-specific enolase, squamous cell carcinoma antigen) were all within normal limits. Immunology testing revealed normal complement C3, weakly positive antinuclear antibody immunoglobulin G, and negative anti-neutrophil cytoplasmic antibody. Lung biopsy tissue obtained under ultrasound-guided bronchoscopy showed no abnormalities on next-generation sequencing (NGS).

Bronchoalveolar lavage fluid galactomannan test was negative; cell differential showed decreased alveolar macrophages (51%) and increased neutrophils (34%). Lavage fluid NGS detected *Streptococcus pneumoniae* and *Haemophilus influenzae*.

Imaging findings

Chest CT demonstrated a mass in the left lower lobe, left supraclavicular and mediastinal lymphadenopathy, and bilateral diffuse microcystic opacities (Figure 1). Whole-body ^{18}F-FDG positron emission tomography (PET)/CT showed a mass in the left lower lobe adjacent to the mediastinum with occlusion of the superior (dorsal) segmental bronchus and increased FDG uptake, most consistent with a primary pulmonary malignancy with surrounding obstructive pneumonia, although inflammatory granulomatous disease could not be entirely excluded. Enlarged lymph nodes, partially confluent, with increased FDG uptake were observed in the left supraclavicular region, bilateral hila, and mediastinum, consistent with lymph node metastasis. Multiple solid nodules and ring-like/irregular cystic lesions were scattered in both lungs, some showing increased FDG uptake, highly suspicious for intrapulmonary metastasis. In addition, minor infectious changes (predominantly in the right upper lobe), left pleural thickening with traction, and coronary artery calcification were noted. Mildly increased FDG uptake in the gastric cardia and lesser curvature, left hepatic lobe, and prostate, together with degenerative spinal changes and

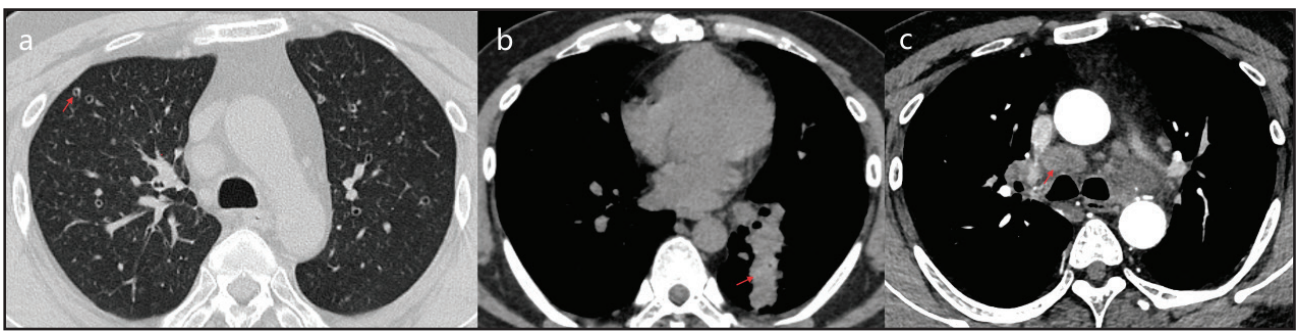

Figure 1. *Baseline chest CT. (a) Lung window showing widespread bilateral multiple thin-walled cystic lesions. (b and c) Mediastinal window showing a left lower lobe mass and mediastinal lymphadenopathy.*

altered bone density of the right eighth rib, was considered most likely inflammatory, reactive, or old lesions; no definitive distant metastasis was identified.

Brain magnetic resonance imaging (MRI) (unenhanced and contrast-enhanced) revealed no abnormal signal intensity or pathological enhancement, and no evidence of intracranial metastasis was detected.

Histopathological findings

Endobronchial ultrasound-guided transbronchial needle aspiration (EBUS-TBNA) targeting the lesion in the superior segment of the left lower lobe yielded only focal atypical epithelial hyperplasia, inconclusive for malignancy. To further clarify the diagnosis, percutaneous lung biopsy and lymph node biopsy were performed. Histology of the left lower lobe tissue revealed several free-floating clusters of atypical epithelial cells; immunohistochemistry showed thyroid transcription factor-1 (TTF-1) (+), Napsin-A (+), p40 (–), synaptophysin (–), diffuse p53 positivity, and a Ki-67 labeling index of approximately 30%, consistent with lung adenocarcinoma (Figure 2). Biopsy of the station 7 (subcarinal) lymph node demonstrated metastatic adenocarcinoma with the immunophenotype (TTF-1 [+], Napsin-A [+], p40 [–]), and biopsy of the station 4R (right lower paratracheal) lymph node also showed metastatic adenocarcinoma, consistent with a pulmonary primary (Figure 3). Fine-needle aspiration of the left supraclavicular lymph node revealed clusters of cells with large, hyperchromatic, atypical nuclei; in combination with the lung biopsy findings and immunohistochemistry (pancytokeratin [+], Napsin-A [+]), metastatic adenocarcinoma was favored. Programmed death-ligand 1 immunohistochemistry (DAKO 22C3 pharmDx) showed a tumor proportion score of 10% (low-level expression), with a combined positive score of 10.

Genetic testing

NGS was performed on genomic deoxyribonucleic acid extracted from the formalin-fixed paraffin-embedded tissue of the percutaneous biopsy of the left lower lobe, using a 56-gene lung cancer–related panel (ADICON Diagnostics, Hangzhou, China). Target regions were captured by hybridization and sequenced on a high-throughput sequencing platform, with a mean target-region coverage of 4079.61× and 100.0% target-region coverage (overall quality Grade A). Sequence data were aligned to the human reference genome (hg19/GRCh37), and variants were annotated according to Human Genome Variation Society nomenclature and classified according to Association for Molecular Pathology/American Society of Clinical Oncology/College of American Pathologists guidelines. No matched normal sample was sequenced; variants were interpreted in a tumor-only context. The assay detected an epidermal growth factor receptor (EGFR) exon 19 in-frame deletion, p.Leu747_Pro753delinsSer (c.2240_2257del; NM_005228.5), with a variant allele frequency (VAF) of 15.1%, and a TP53 missense mutation, p.Ile195Thr (c.584T>C; NM_000546.5), with a VAF of 24.84%. No additional actionable alterations were detected in ALK, ROS1, BRAF, KRAS, MET, RET, NTRK1, or ERBB2. An NFE2L2 missense variant, p.Ile22Val (c.64A>G; NM_006164.5), with a VAF of 52.36%, was classified as a variant of uncertain clinical significance; given the VAF of approximately 50% and the absence of matched normal testing, a germline origin could not be excluded. Microsatellite instability was not detected (the tumor was microsatellite-stable), and tumor mutational burden was not assessed by this focused panel.

Treatment and follow-up

Anti-infective therapy with moxifloxacin (0.4 g intravenously once daily) for 10 days administered at the outside hospital was ineffective. After admission, bronchoalveolar

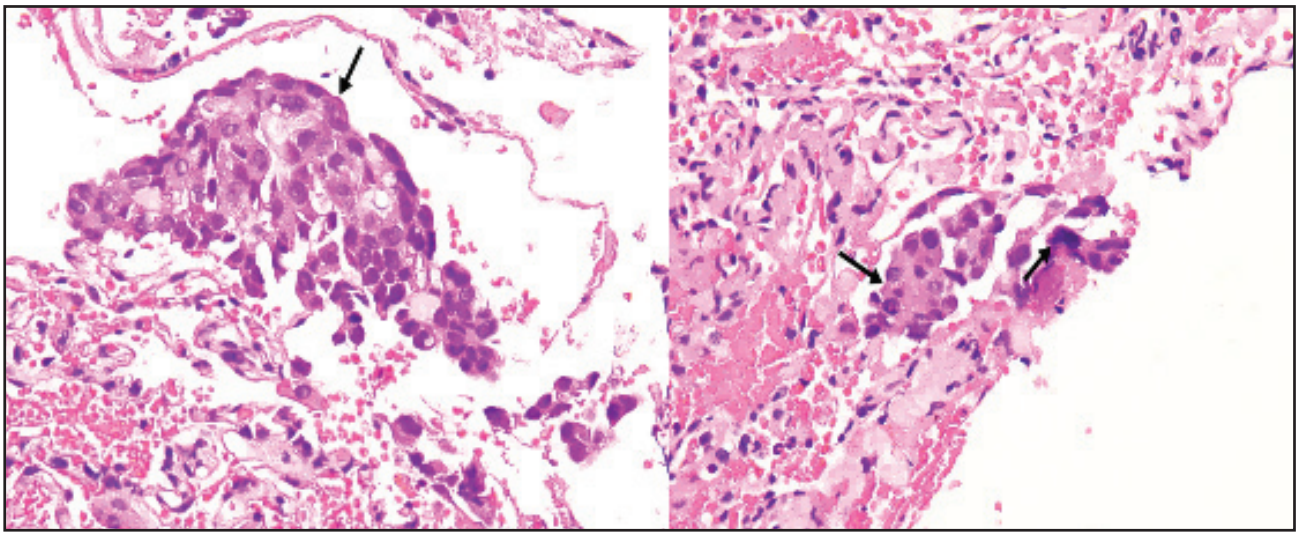

Figure 2. *Lung puncture biopsy of the left lower lobe dorsal segment shows nests of atypical epithelial cells with obvious cellular atypia, consistent with lung adenocarcinoma (hematoxylin–eosin staining, objective ×20).*

lavage fluid metagenomic next-generation sequencing (mNGS) identified pathogenic organisms and, in view of the accompanying imaging findings, therapy was switched to cefoperazone–sulbactam (1 g intravenously, twice daily) for 10 days. His fever and sputum production resolved; C-reactive protein decreased from 45.22 to 6.31 mg/l and the white blood cell count from 6.86 × 10^9/l to 4.33 × 10^9/l, while procalcitonin remained within the normal range. However, the pulmonary lesions persisted on repeat imaging.

Based on the histopathological and molecular findings, the patient was diagnosed with lung adenocarcinoma of the left lower lobe (cT3N3M1a, stage IVA, according to the 8th edition TNM classification). The M1a category was assigned on the basis of radiological suspicion of contralateral intrapulmonary metastasis (the bilateral microcystic lesions) rather than histological confirmation; brain MRI and whole-body PET/CT showed no evidence of other distant metastases. Given the EGFR exon 19 deletion identified by NGS, first-line osimertinib (80 mg once daily) was initiated.

Follow-up chest CT after 1 month of treatment (January 16, 2026) showed a reduction of the left lower lobe lesion, partial regression or disappearance of the bilateral microcystic lesions, and decreased mediastinal lymphadenopathy (Figure 4). These improvements were sustained on

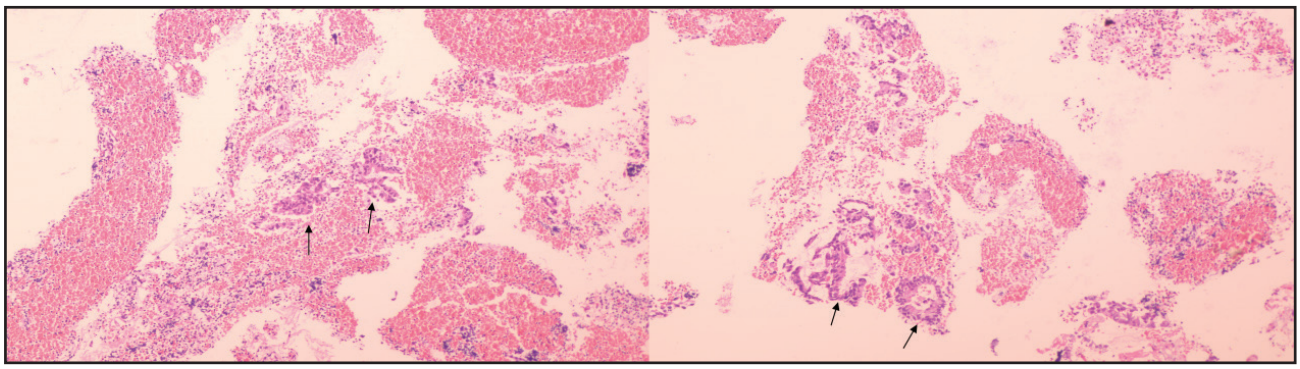

Figure 3. *Histopathological findings of the percutaneous lymph node biopsy demonstrating metastatic adenocarcinoma (hematoxylin and eosin staining, objective ×4).*

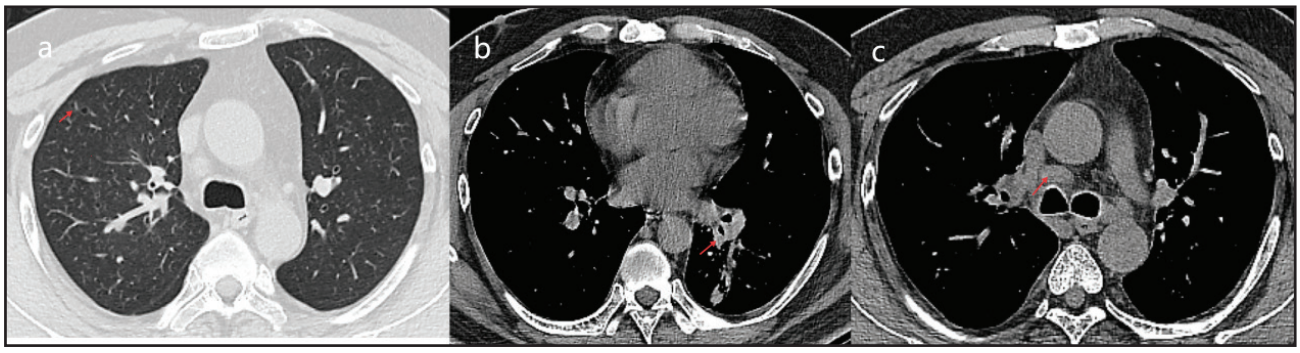

Figure 4. *Chest CT (January 16, 2026). (a) Lung window showing partial reduction or disappearance of the bilateral multiple small cystic lesions. (b and c) Mediastinal window showing reduction of the left lower lobe mass and of the mediastinal lymphadenopathy compared with baseline.*

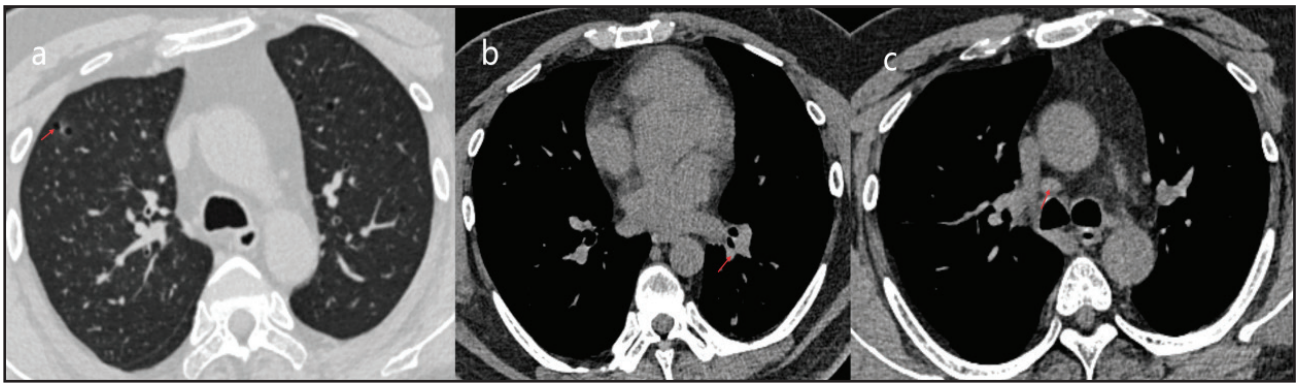

Figure 5. *Chest CT (April 15, 2026). (a) Lung window showing stable bilateral small cystic lesions. (b and c) Mediastinal window showing further reduction of the left lower lobe mass, with essentially stable mediastinal lymph nodes.*

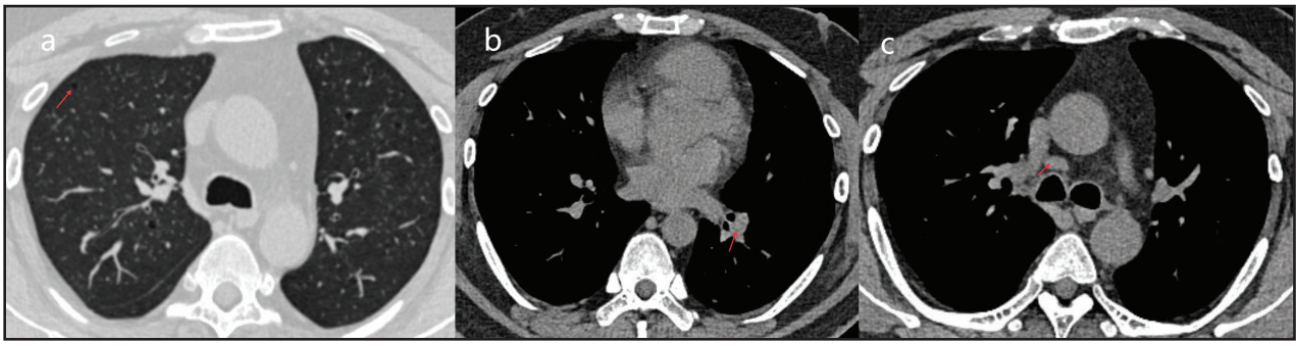

Figure 6. *Chest CT (August 29, 2026). (a) Lung window showing stable bilateral small cystic lesions. (b and c) Mediastinal window showing continued reduction of the left lower lobe mass, with stable mediastinal lymph nodes.*

Table 1. *RECIST 1.1 response during osimertinib treatment: target-lesion sum 71.39→39.33 (–44.9%)→34.14 (–52.2%)→30.00 mm (–58.0%) at baseline and 1, 4, and 9 months (ongoing PR); non-target microcystic lesions 5.0→3.82 mm; no new lesions.*

TIME POINT	LEFT LOWER LUNG MASS (LONGEST DIAMETER, MM)	MEDIASTINAL LYMPH NODE (SHORT AXIS, MM)	SUM OF TARGET LESIONS (MM)	CYSTIC LESION (MM)
Baseline (December 2, 2025)	53.65	17.74	71.39	5.00
Follow-up 1 (January 16, 2026)	30.99	8.34	39.33	4.15
Follow-up 2 (April 15, 2026)	26.31	7.83	34.14	3.91
Follow-up 3 (August 29, 2026)	22.38	7.62	30.00	3.82

restaging CT at 4 months (April 15, 2026; Figure 5) and 9 months (August 29, 2026; Figure 6).

Treatment response was assessed according to Response Evaluation Criteria in Solid Tumors (RECIST) 1.1. The primary tumor in the left lower lobe (longest diameter) and a representative mediastinal lymph node (short-axis diameter) were selected as target lesions; the bilateral microcystic lesions were classified as non-target lesions, as cystic lesions are not measurable under RECIST 1.1. Baseline chest CT (December 2, 2025) demonstrated a sum of target-lesion diameters of 71.39 mm (primary lesion, 53.65 mm; lymph node, 17.74 mm). On the first restaging CT (January 16, 2026, 1 month after treatment initiation), the sum had decreased to 39.33 mm (−44.9% from baseline), consistent with a partial response (PR). The response was maintained on subsequent restaging: 34.14 mm (−52.2%) at 4 months (April 15, 2026) and 30.00 mm (−58.0%) at 9 months (August 29, 2026), confirming an ongoing PR. The non-target microcystic lesions regressed progressively (a representative lesion decreased from 5.0 to 3.82 mm), and no new lesions were identified (Table 1). No significant adverse events, radiological progression, or evidence of acquired resistance has been observed to date. The patient continues osimertinib 80 mg once daily under regular radiological surveillance.

Discussion

Bilateral multiple microcystic pulmonary lesions in patients with lung adenocarcinoma are clinically rare and are easily confused with infection, bronchiectasis, or cystic lung diseases [7,9], which may lead to misdiagnosis. The present case involves a 35-year-old welder with several recognized risk factors, including smoking, long-term occupational welding-fume exposure, and a family history of lung cancer. The diagnosis of lung adenocarcinoma with an EGFR exon 19 deletion and a TP53 co-mutation was confirmed by pathology and genetic testing of the primary left lower lobe lesion and metastatic lymph nodes. Notably, after 1 month of osimertinib treatment, the bilateral microcystic lesions showed significant regression and continued to improve through 9 months of follow-up, consistent with a malignant (metastatic) etiology of these lesions and highlighting the therapeutic value of timely targeted therapy; nevertheless, histopathological confirmation of these cystic lesions was not obtained, and they remain highly suspicious for intrapulmonary metastasis rather than proven metastases.

Lung cancer is uncommon in young adults, and lung adenocarcinoma is the predominant histology in this age group; the incidence in patients under 40 years is approximately 1%–5% of all lung cancers [10]. Young patients often lack typical symptoms, which delays diagnosis. Our patient was only 35 years old – far younger than the usual peak onset age of 50–70 years. He had multiple risk factors: a long history of smoking (17 pack-years), occupational welding exposure (17 years, IARC Group 1 carcinogen), and a family history of lung cancer. Smoking is a well-established carcinogen, benzo[a]pyrene in cigarette smoke directly damages airway epithelial cells [11]. Welding fumes are classified as a Group 1 carcinogen by the IARC and contain several potentially carcinogenic constituents, including hexavalent chromium, nickel, iron oxides, and polycyclic aromatic hydrocarbons [8,12]. However, the co-existence of these risk factors in a single

patient does not establish a causal link to the development of EGFR-mutated lung adenocarcinoma. Whether the EGFR exon 19 deletion identified in this patient is related to his occupational or tobacco exposure remains speculative and would require further molecular epidemiological studies.

The most prominent imaging feature in this case is bilateral multiple microcystic opacities. Several mechanisms have been proposed in the literature to explain cyst formation in pulmonary metastases, including (a) endobronchial tumor infiltration causing luminal stenosis and a check-valve effect with overdistension of the distal alveoli, (b) tumor growth along the alveolar walls with destruction of the alveolar structure and fusion into cystic spaces, and (c) tumor necrosis and liquefaction with subsequent expulsion via the airways, leaving a cyst wall [13]. The mechanisms proposed for microcyst formation are speculative, and none could be confirmed in the present case, as the microcystic lesions were not biopsied. The evidence available in our patient was indirect: some of the cystic lesions showed increased FDG uptake on PET/CT, suggesting metabolically active tumor tissue in the cyst wall or adjacent parenchyma, and the lesions regressed in parallel with the primary tumor under osimertinib. These findings support a neoplastic origin of the microcystic lesions but do not permit discrimination among the proposed mechanisms; in particular, whether the check-valve mechanism contributed could not be determined without airway or histological assessment.

On imaging, multiple cystic or cavitary lung lesions carry a broad differential diagnosis. First, infectious etiologies warrant consideration. In this patient, productive cough, fever, and elevated inflammatory markers were consistent with infection, and bronchoalveolar lavage mNGS identified *S. pneumoniae* and *H. influenzae*, which – in the setting of obstructive pneumonia distal to the tumor – were regarded as true pathogens rather than colonization. This pneumonia resolved with cefoperazone–sulbactam, with normalization of inflammatory markers, whereas the microcystic lesions persisted and regressed only after osimertinib, indicating that infection and malignancy coexisted, but the cysts themselves were not of infectious origin. *Pneumocystis jirovecii* pneumonia, septic emboli, tuberculosis, and fungal infection were further excluded by the intact immune status and negative cultures. Second, cystic lung diseases such as pulmonary Langerhans cell histiocytosis (PLCH) and lymphangioleiomyomatosis (LAM) warrant consideration. PLCH predominantly affects young to middle-aged smokers aged 20–40 years, with irregular cysts predominating in the upper and mid lung zones [14]. LAM occurs almost exclusively in women of childbearing age, with uniform, round, thin-walled cysts often associated with renal angiomyolipomas [15]. The patient's sex, age, and imaging features are inconsistent with either PLCH or LAM. Other diffuse cystic lung diseases – Birt–Hogg–Dubé syndrome, lymphocytic interstitial pneumonia/Sjögren syndrome, desquamative interstitial pneumonia, and amyloidosis/light-chain deposition disease – as well as cyst-mimicking lesions (emphysema, honeycombing, cystic bronchiectasis, pneumatoceles) were excluded by cyst morphology, distribution, and the absence of autoimmune, cutaneous, or renal involvement [16–17]. Third, among neoplastic etiologies, lung adenocarcinoma associated with cystic airspaces and cystic pulmonary metastases are the most relevant: multiple and irregular cystic airspaces independently predict invasive adenocarcinoma [18], and new thin-walled cysts in a patient with known malignancy warrant concern for metastasis [16]. In this patient, the FDG uptake within the lesions and their parallel shrinkage with the primary tumor on osimertinib support a metastatic origin.

Molecular features

This case was characterized by an EGFR exon 19 deletion (p.Leu747_Pro753delinsSer) with concurrent TP53 (p.Ile195Thr) and NFE2L2 (p.Ile22Val) variants. The NFE2L2 variant's high allele frequency (approximately 52%) raises the possibility of a germline origin, although germline testing was not performed in this case. EGFR exon 19 deletion is the most common EGFR-sensitizing mutation in lung adenocarcinoma and confers high sensitivity to third-generation EGFR tyrosine kinase inhibitors (TKIs). Osimertinib is a third-generation EGFR-TKI that targets both EGFR-sensitizing mutations and the T790M resistance mutation and efficiently penetrates the blood–brain barrier [19]. TP53 is the most frequently co-mutated gene with EGFR in NSCLC, and concurrent TP53 alterations have been associated with genomic instability and, in some series, earlier development of resistance to EGFR-TKIs [20]. In our patient, the primary tumor and pulmonary lesions showed a PR on first-line osimertinib that was maintained at the 9-month follow-up, indicating that the TP53 co-mutation did not preclude a response in this individual; however, this single-case observation does not permit general prognostic conclusions.

Conclusion

This case highlights that bilateral multiple microcystic pulmonary lesions in a young patient with risk factors should raise suspicion of metastatic involvement from lung adenocarcinoma, prompting timely pathological biopsy and genetic testing for timely diagnosis. In this patient, 9 months of osimertinib therapy achieved a sustained radiological response despite the concurrent TP53 mutation, suggesting that TP53 co-mutation did not preclude response in this patient, although this single case cannot be generalized.

What's new?

Diffuse cystic lung metastases are a rare radiological manifestation, previously reported predominantly in older patients with advanced adenocarcinoma. The authors report a case of a 35-year-old Chinese male welder with bilateral diffuse microcystic pulmonary metastases from lung adenocarcinoma harboring an EGFR exon 19 deletion with concurrent TP53 and NFE2L2 mutations. This case is notable for (1) The unusual, previously not well-described combination of diffuse cystic metastases with young age, long-term welding exposure, and a strong family history of lung cancer; (2) The diagnostic pitfall of cystic lesions initially attributed to infection, resolved only after failed antibiotic therapy; and (3) A rapid, ongoing radiological response (−58% by RECIST 1.1) to first-line osimertinib despite TP53 co-mutation. The report underscores that diffuse cystic lung disease in a young patient with risk factors warrants early malignancy workup.

List of Abbreviations

CPS	Combined positive score
CT	Computed tomography
EBUS-TBNA	Endobronchial ultrasound-guided transbronchial needle aspiration
EGFR	Epidermal growth factor receptor
IARC	International Agency for Research on Cancer
LAM	Lymphangioleiomyomatosis
mNGS	Metagenomic next-generation sequencing
NGS	Next-generation sequencing
NSCLC	Non-small cell lung cancer
PLCH	Pulmonary Langerhans cell histiocytosis
PR	Partial response
RECIST	Response Evaluation Criteria in Solid Tumors
TKI	Tyrosine kinase inhibitor
TNM	Tumor-node-metastasis
VAF	Variant allele frequency

Competing interests

The authors declare that they have no competing interests.

Funding

This work was supported by the National Natural Science Foundation of China (82500066), the Natural Science Foundation Exploration Plan of Wuhan (2025040601020212), and Noncommunicable Chronic Diseases-National Science and Technology Major Project (2026ZD0556204).

Consent for publication

Written informed consent was obtained from the patient for publication of this case report and any accompanying images. A copy of the written consent is available for review by the Editor-in-Chief of this journal.

Ethics approval and consent to participate

This case report was granted an exemption from ethical review by the Institutional Review Board of the Affiliated Hospital of Jianghan University in accordance with institutional policies. Written informed consent was obtained from the patient for participation and for publication of this case report and any accompanying images.

Data availability statement

Not applicable.

Author Details

Qin Jian[1], Di Xu[1], Min Liu, Bingzhu Hu[1], Chenghong Li[1]

1. Department of Pulmonary and Critical Care Medicine, Affiliated Hospital of Jianghan University, Wuhan, Hubei, China.

References

1. Smolarz B, Łukasiewicz H, Samulak D, Piekarska E, Kołaciński R, Romanowicz H. Lung cancer-epidemiology, pathogenesis, treatment and molecular aspect (review of literature). Int J Mol Sci. 2025;26(5):2049. https://doi.org/10.3390/ijms26052049
2. Shong LY, Lam DC. Emerging trends in global lung cancer burden. Semin Respir Crit Care Med. 2025;46(5):409–18. https://doi.org/10.1055/a-2651-0612
3. Sumiya R, Matsunaga T, Suzuki K. Lung cancer in young individuals; risk factors and epidemiology. J Thorac Dis. 2025;17(3):1746–54. https://doi.org/10.21037/jtd-2024-1950
4. Rocca A, Crinò L, Braga L, Salton F, Ruaro B, Confalonieri M, et al. Refining treatment strategies for non-small cell lung cancer lacking actionable mutations: insights from multi-omics studies. Br J Cancer. 2025;133(10):1405–27. https://doi.org/10.1038/s41416-025-03139-6
5. Lohinai Z, Klikovits T, Moldvay J, Ostoros G, Raso E, Timar J, et al. KRAS-mutation incidence and prognostic value are metastatic site-specific in lung adenocarcinoma: poor prognosis in patients with KRAS mutation and bone metastasis. Sci Rep. 2017;7(1):39721. https://doi.org/10.1038/srep39721
6. Tiresse N, Boucaid A, Laamim R, Chafi K, Souhi H. Diffuse bilateral pseudo-cystic pulmonary lesions revealing metastatic lung adenocarcinoma: a case report and literature review. Cureus. 2026;18(2):e103730. https://doi.org/10.7759/cureus.103730
7. Gui XH, Li Y, Yu M, Chen TT, Ding JJ, Huang M, et al. [Imaging features of lung adenocarcinoma with diffuse cystic manifestations: two cases report] [in Chinese]. Zhonghua Jie He He Hu Xi Za Zhi. 2020;43(3):242–4.
8. Loomis D, Dzhambov AM, Momen NC, Chartres N, Descatha A, Guha N, et al. The effect of occupational exposure to welding fumes on trachea, bronchus and lung cancer: a systematic review and meta-analysis from the WHO/ILO joint estimates of the work-related burden of disease and injury. Environ Int. 2022;170:107565. https://doi.org/10.1016/j.envint.2022.107565
9. Gupta N, Vassallo R, Wikenheiser-Brokamp KA, McCormack FX. Diffuse cystic lung disease. Part I. Am J Respir Crit Care Med. 2015;191(12):1354–66. https://doi.org/10.1164/rccm.201411-2094CI
10. Gómez López A, Valipour A, Álvarez Martínez CJ. Lung cancer in young adults. Open Respir Arch. 2025;7(4):100497. https://doi.org/10.1016/j.opresp.2025.100497
11. Fan L, Li W, Ma J, Cheng M, Xie L, Ye Z, et al. Benzo(a)pyrene induces airway epithelial injury through Wnt5a-mediated non-canonical Wnt-YAP/TAZ signaling. Sci Total Environ. 2022;815:151965. https://doi.org/10.1016/j.scitotenv.2021.151965
12. Tavares AM, Viegas S, Louro H, Göen T, Santonen T, Luijten M, et al. Occupational exposure to hexavalent chromium, nickel and PAHs: a mixtures risk assessment approach based on literature exposure data from European countries. Toxics. 2022;10(8):431. https://doi.org/10.3390/toxics10080431
13. Fintelmann FJ, Brinkmann JK, Jeck WR, Troschel FM, Digumarthy SR, Mino-Kenudson M, et al. Lung cancers

associated with cystic airspaces: natural history, pathologic correlation, and mutational analysis. J Thorac Imaging. 2017;32(3):176–88. https://doi.org/10.1097/RTI.0000000000000265

14. Ahuja J, Kanne JP, Meyer CA, Pipavath SN, Schmidt RA, Swanson JO, et al. Histiocytic disorders of the chest: imaging findings. Radiographics 2015;35(2):357–70. https://doi.org/10.1148/rg.352140197
15. Pallisa E, Sanz P, Roman A, Majó J, Andreu J, Cáceres J. Lymphangioleiomyomatosis: pulmonary and abdominal findings with pathologic correlation. Radiographics 2002;22(Spec No suppl_1):S185–98. https://doi.org/10.1148/radiographics.22.suppl_1.g02oc13s185
16. Singh P, Verma AK, Pandey G. Diffuse cystic lung diseases: imaging spectrum and diagnostic approach using high-resolution computed tomography. Lung India. 2022;39(6):553–61. https://doi.org/10.4103/lungindia.lungindia_44_22
17. Cabeza Martínez B, Giménez Palleiro A, Mazzini Florindez SP. Cystic lung disease. Radiologia (Engl Ed). 2022;64 Suppl 3:265–76. https://doi.org/10.1016/j.rxeng.2022.09.005
18. Zhu H, Zhang L, Huang Z, Chen J, Sun L, Chen Y, et al. Lung adenocarcinoma associated with cystic airspaces: predictive value of CT features in assessing pathologic invasiveness. Eur J Radiol. 2023;165:110947. https://doi.org/10.1016/j.ejrad.2023.110947
19. Cross DA, Ashton SE, Ghiorghiu S, Eberlein C, Nebhan CA, Spitzler PJ, et al. AZD9291, an irreversible EGFR TKI, overcomes T790M-mediated resistance to EGFR inhibitors in lung cancer. Cancer Discov. 2014;4(9):1046–61. https://doi.org/10.1158/2159-8290.CD-14-0337
20. Canale M, Andrikou K, Priano I, Cravero P, Pasini L, Urbini M, et al. The role of TP53 mutations in EGFR-mutated non-small-cell lung cancer: clinical significance and implications for therapy. Cancers (Basel). 2022;14(5):1143. https://doi.org/10.3390/cancers14051143

Summary of the case

1	Patient (gender, age)	35 years, male
2	Final diagnosis	Lung adenocarcinoma (left lower lobe), cT3N3M1a, stage IVA
3	Symptoms	Cough, blood-streaked sputum, exertional dyspnea
4	Medications	Osimertinib 80 mg once daily
5	Clinical Procedure	Percutaneous lung biopsy, lymph node biopsy, EBUS-TBNA, genetic testing
6	Specialty	Thoracic Oncology / Pulmonary Medicine